

# Atomic Force Microscopy Analysis of EPPS-Driven Degradation and Reformation of Amyloid- $\beta$ Aggregates

Wonseok Lee<sup>a,1</sup>, Sang Won Lee<sup>b,1</sup>, Gyudo Lee<sup>b,\*</sup> and Dae Sung Yoon<sup>b,\*</sup>

<sup>a</sup>*Department of Biomedical Engineering, Yonsei University, Wonju, Korea*

<sup>b</sup>*School of Biomedical Engineering, Korea University, Seoul, Korea*

Accepted 15 January 2018

**Abstract.** Amyloid- $\beta$  (A $\beta$ ) peptides can be aggregated into  $\beta$ -sheet rich fibrils or plaques and deposited on the extracellular matrix of brain tissues, which is a hallmark of Alzheimer's disease. Several drug candidates have been designed to retard the progression of the neurodegenerative disorder or to eliminate toxic A $\beta$  aggregates. Recently, 4-(2-Hydroxyethyl)-1-piperazinepropanesulfonic acid (EPPS) has emerged as a promising drug candidates for elimination of toxic A $\beta$  aggregates. However, the effect of EPPS on the degradation of A $\beta$  aggregates such as fibrils has not yet been fully elucidated. In this article, we investigate the EPPS-driven degradative behavior of A $\beta$  aggregates at the molecular level by using high-resolution atomic force microscopy. We synthesized A $\beta$  fibrils and observed degradation of fibrils following treatment with various concentrations (1–50 mM) of EPPS for various time periods. We found that degradation of A $\beta$  fibrils by EPPS increased as a function of concentration and treatment duration. Intriguingly, we also found regeneration of A $\beta$  aggregates with larger sizes than original aggregates at high concentrations (10 and 50 mM) of EPPS. This might be attributed to a shorter lag phase that facilitates reformation of A $\beta$  aggregates in the absence of clearance system.

**Keywords:** A $\beta$  aggregates, Alzheimer's disease, amyloid- $\beta$ , atomic force microscopy, 4-(2-Hydroxyethyl)-1-piperazinepropanesulfonic acid (EPPS), fibril degradation

## INTRODUCTION

The production and deposition of amyloid- $\beta$  peptide (A $\beta$ ) are the hallmarks of Alzheimer's disease (AD) [1–3]. A $\beta$  peptides derived from the amyloid- $\beta$  protein precursor can aggregate into insoluble amyloid aggregates such as A $\beta$  oligomers, fibrils, and plaques [1, 2, 4]. There have been many attempts to eliminate A $\beta$  aggregates in order to alleviate or cure AD. For example, plasma jets [5], laser radiation

[6], ultrasonication [7], thermal energy [8], and drugs [9, 10] have been tried to remove A $\beta$  aggregates. Of these approaches, the development of drugs that can degrade the A $\beta$  aggregates has been the focus of research because these agents offer the most realistic way to reach A $\beta$  aggregates inside the body.

Most drugs targeting A $\beta$  can be categorized by three different mechanisms: 1) reducing the production of the A $\beta$  peptides by using inhibitors such as  $\gamma$ -secretase or  $\beta$ -secretase; 2) eliminating A $\beta$  monomers and oligomers before forming A $\beta$  fibrils or plaques in the initial formation stages; 3) disrupting A $\beta$  aggregates in the brain [4, 11, 12]. Despite these methods, there have been a few

<sup>1</sup>These authors contributed equally to this work.

\*Correspondence to: Dae Sung Yoon and Gyudo Lee, School of Biomedical Engineering, Korea University, Seoul 02841, Korea. E-mails: dsyoon@korea.ac.kr; leegyudo@gmail.com

reports on drug candidates that could possibly cure AD. So far, drug candidate (4-(2-Hydroxyethyl)-1-piperazinepropanesulfonic acid (EPPS)) have been identified, and tested for effectiveness in degradation of A $\beta$  aggregates *in vitro* or *in vivo* [13]. In particular, EPPS is believed to be the most promising drug candidate offering the hope of a cure for AD. Specifically, Kim et al. recently reported highly effective EPPS-driven degradation of toxic A $\beta$  aggregates *in vitro* and *in vivo* [14]. However, despite its importance, the detailed mechanism of EPPS-driven A $\beta$  degradation at the molecular level has not yet been fully elucidated.

In this study, we demonstrated the EPPS-driven degradation of A $\beta$ <sub>1-42</sub> amyloid aggregates *in vitro* using atomic force microscopy (AFM). As a powerful nanomechanical imaging technique, AFM has been used in investigating amyloid formation and polymorphism *in vitro* [15, 16]. AFM analysis offered abundant and visual data regarding the degradation of A $\beta$ <sub>1-42</sub> amyloid aggregates at different EPPS concentrations (1–50 mM) and treatment times (0–3 days). Our results shed light on drug discovery and *in vitro* examination at the molecular level of EPPS for the prevention and treatment of AD.

## MATERIALS AND METHODS

### *Preparation of A $\beta$ and EPPS treatment*

Lyophilized amyloid- $\beta$  42 (A $\beta$ <sub>1-42</sub>) peptide (TOCRIS, UK) was dissolved in 1,1,1,3,3,3-Hexafluoro-2-Propanol (HFIP, Sigma-Aldrich, St. Louis, MO, USA). The peptide (1 mM) was distributed in micro-centrifuge tubes and then the peptide solution was dried overnight. The peptide transformed into a thin film at the bottom of the tubes. The film was dissolved in dimethyl sulfoxide (Sigma-Aldrich, St. Louis, MO, USA) and the concentration became 5 mM. To synthesis of A $\beta$  fibrils, the prepared solution was resuspended in a 10 mM hydrochloric acid (HCl) solution. The final concentration of the A $\beta$  solution was 50  $\mu$ M. The solution was incubated in an oil bath at 37°C for 3 days. We then dialyzed the solution against distilled water for 60 h by using 50 kDa dialysis membranes (Biovision Inc, USA). The incubated A $\beta$  solution and 1–50 mM of EPPS (Sigma-Aldrich, USA) solution mixed at a volume ratio of (1:1) and then the mixed solution was incubated for 1–3 days at 37°C.

### *AFM imaging of A $\beta$ aggregates with EPPS treatment*

The A $\beta$  solution (50  $\mu$ L) was deposited on clean mica for 5 min and then washed 3 times with 100  $\mu$ L distilled water (H<sub>2</sub>O) and gently dried under pure nitrogen gas [17–19]. AFM images of A $\beta$  fibrils with or without EPPS were acquired using a Multimode V instrument (Veeco, USA) and an Innova (Bruker, USA) operated in tapping mode AFM in the air and at room temperature. To minimize the noise from the air, an AFM housing system was used. A silicon cantilever (TESP-V2, Bruker, USA) was used and scan rate was 0.5 Hz. The resonance frequency of the cantilever for imaging was  $\sim$ 300 kHz. All AFM imaging areas were 100  $\mu$ m<sup>2</sup>. The acquired images were evaluated using NanoScope analysis software 1.8 version. Cross-sectional analysis and calculation of surface roughness were conducted using the same software [7, 17–19].

## RESULTS AND DISCUSSIONS

### *EPPS-driven degradation of A $\beta$ fibrils at low concentration of A $\beta$ solution*

We synthesized 50  $\mu$ M A $\beta$ <sub>1-42</sub> amyloid fibrils to observe the degradation of amyloid fibrils by treatment with drug candidates (Fig. 1a). We note that A $\beta$  fibril formation was conducted in a strongly acidic solution (pH 2) for fast and stable fibrillation [7, 17–20]. Meanwhile, based on a previous report that said that EPPS works well at pH 7.3–8.7 [13, 14], we dialyzed the prepared A $\beta$  solution to replace the acidic solution with distilled water (H<sub>2</sub>O) (Fig. 1b). There was no significant change in both morphology and density of A $\beta$  fibrils before and after dialysis. The A $\beta$  fibrils are well dispersed in the solution. In the first place, we thought that the 50  $\mu$ M A $\beta$  is too dense to study the effects of EPPS on the degradation of the A $\beta$  fibrils. Thus, we diluted the A $\beta$  solution from 50 to 5  $\mu$ M, resulting in distinct individual A $\beta$  fibrils, as seen on AFM images (under current experimental conditions) distinctively in our AFM imaging condition (Fig. 1c).

We treated a A $\beta$  solution (5  $\mu$ M) with 5 and 10 mM of EPPS, respectively, for different incubation times (6, 12, and 24 h, respectively) at 37°C and we investigated the changes by AFM (Fig. 1d, e). As expected, EPPS directly binds on the preformed A $\beta$  aggregates and works well, i.e., increased degradation of A $\beta$  fibrils with rising EPPS concentrations and

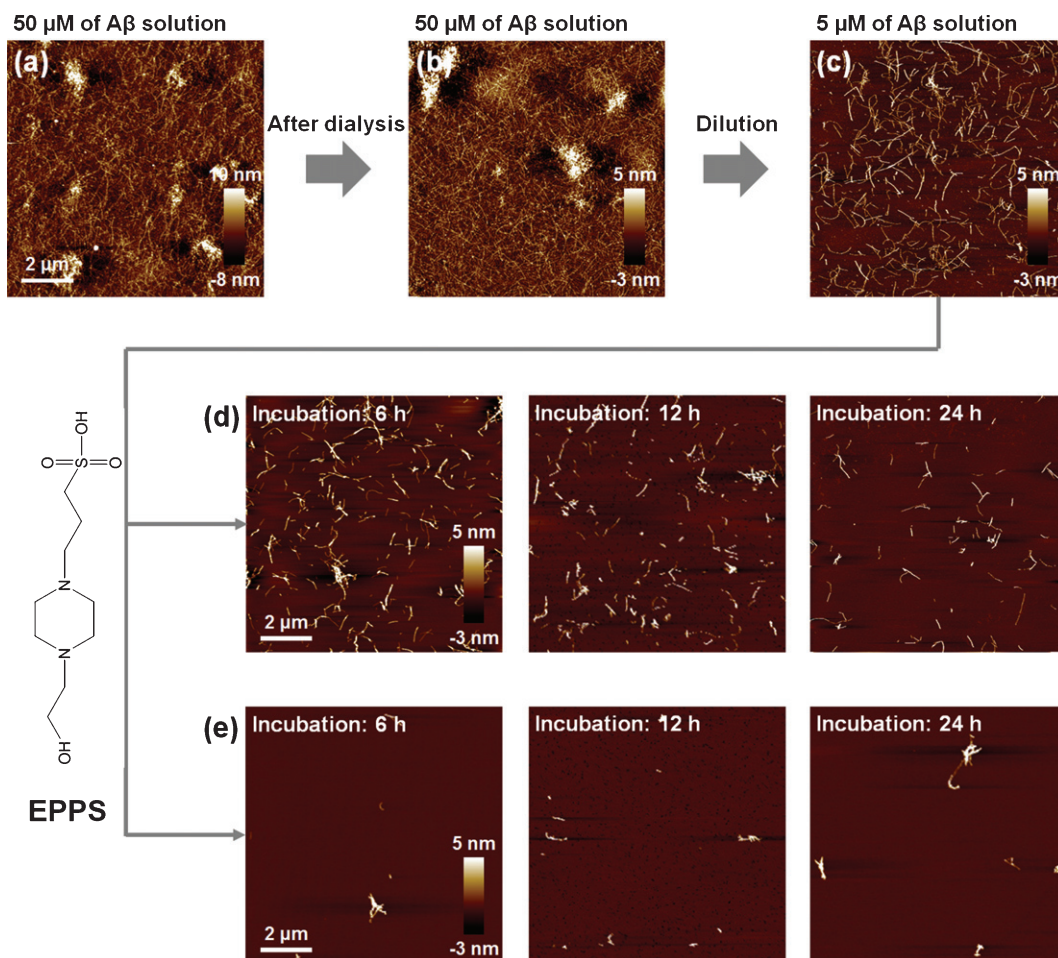


Fig. 1. AFM images of A $\beta$  fibrils. (a) 50  $\mu$ M of A $\beta$  fibrils in 10 mM of hydrochloric acid (HCl) solution (approximately adjusted to pH 2). (b) 50  $\mu$ M of A $\beta$  fibrils after dialysis in distilled water (H $_2$ O) for 60 h. (c) 5  $\mu$ M of A $\beta$  fibrils diluted from (b). (d, e) AFM images of 5 mM (d) and 10 mM (e) of EPPS treated A $\beta$  fibrils with different incubation times (6–24 h).

incubation times. Consistent with previous reports, increased incubation time in the presence of EPPS led to a reduction in the densities and lengths of fibrils [14]. Moreover, a drastic degradation of A $\beta$  fibrils was observed at 10 mM of EPPS; incubation with 10 mM EPPS for 6 h seemed more effective than the results obtained following a 24 h-incubation time in the presence of 5 mM of EPPS. This implied that the higher concentration of EPPS was more critical than the longer incubation time for A $\beta$  degradation. In this context, we conducted the concentration test with 1–50 mM of EPPS against A $\beta$  fibrils (5  $\mu$ M) for 1 day (Fig. 2a-d). We found that treatment in the presence of a higher concentration of EPPS led to the decomposition of more fibrils. In specific, we observed that the 5 mM of EPPS is more effective in degradation of A $\beta$  fibrils than 1 mM of EPPS

treatment. For quantitative analysis of A $\beta$  fibrils, we measured the height of A $\beta$  fibrils with AFM images (Fig. 2e). The heights of A $\beta$  fibrils treated with 1 mM of EPPS were changed from  $3.13 \pm 1.80$  (non-treated A $\beta$  fibrils) to  $3.71 \pm 2.48$  nm (gray line). Higher concentrations of EPPS (5 and 10 mM) treatment slightly diminished the heights of A $\beta$  fibrils. Following treatment with 50 mM of EPPS, the height of A $\beta$  fibrils abruptly increased from  $3.13 \pm 1.80$  to  $6.90 \pm 3.54$  nm. Aggregates of A $\beta$  fibrils appeared on the AFM images (Fig. 2c, d). This increase of the height of degraded A $\beta$  fibrils may be attributed to the increase in the number of free ends through breakage of the fibril [21]. Concretely, as the number of free ends of degraded A $\beta$  fragment increases, they can be aggregated via chemical functional groups in free ends. This trend was consistent with the results

of the surface roughness analysis (Fig. 2f). As the EPPS concentration (1–50 mM) used to treat A $\beta$  fibrils increased, we found that the surface roughness decreased from  $0.52 \pm 0.04$  to  $0.20 \pm 0.15$  nm. The trend towards a lower surface roughness showed that A $\beta$  fibrils were diminished by EPPS treatment.

Interestingly, small aggregates that could be A $\beta$  fragments were still found after incubation at 50 mM of EPPS—a concentration that was 10,000-fold higher than the prepared A $\beta$  solution (5  $\mu$ M). Seemingly, this result indicated that EPPS could not perfectly remove A $\beta$  fibrils, albeit at a very high concentration. It is well known that very small amounts of amyloid fragments act as seed nuclei that can facilitate amyloid reformation much more rapidly than initial amyloid formation [7]. Even though such reformed amyloid aggregates could not elicit directly cytotoxicity for neurons in the brain, the facilitated amyloid aggregation is likely to make the prognosis worse in the treatment of Alzheimer's disease [22].

#### *EPPS-driven degradation of A $\beta$ fibrils at high concentration of A $\beta$ solution*

To investigate the EPPS-driven degradation of A $\beta$  fibrils at high concentration of A $\beta$  solution, we used 50  $\mu$ M A $\beta$  solutions (Fig. 1b) that are treated with 1 mM EPPS for 3 days. There were several A $\beta$  aggregates in the A $\beta$  fibril sample (50  $\mu$ M) in the absence of EPPS. As the incubation time of EPPS increased, the aggregates seemed to be degraded (Fig. 3a-c). Moreover, the density of A $\beta$  fibrils declined (see AFM images), suggesting that EPPS worked. Based on the cross-section profile (Fig. 3d-f), we confirmed that not only the heights of the A $\beta$  aggregates, but also the overall densities of A $\beta$  fibrils, decreased with increasing incubation times (from 1 to 3 days). Consistent with observations by AFM, we concluded that the A $\beta$  fibrils declined and that the A $\beta$  aggregates were destroyed.

For investigating the high concentration effect, we considered the higher concentration of EPPS (1–50 mM) on A $\beta$  fibrils (50  $\mu$ M) for 1 day (Fig. 4). As seen in Fig. 3a, the A $\beta$  aggregates and densities of A $\beta$  fibrils were slightly decreased by 1 mM of EPPS treatment of more than 50  $\mu$ M of A $\beta$  fibrils (Fig. 4a). Interestingly, we found that A $\beta$  fibrils were more destroyed in the presence of 5 mM of EPPS (Fig. 4b), but at higher EPPS (>5 mM), the large-sized (4–10  $\mu$ m) A $\beta$  aggregates were observed at 10 and 50 mM of EPPS (Fig. 4c and

d). The heights of fibrils and the aggregates tended to increase from  $2.57 \pm 1.39$  to  $14.24 \pm 3.30$  nm, depending on the EPPS concentration (5–50 mM) (Fig. 4e). Similarly, the surface roughness increased in accordance with the high concentration of EPPS (5–50 mM);  $0.31 \pm 0.05$ ,  $0.60 \pm 0.49$ , and  $3.60 \pm 0.44$  nm, respectively (Fig. 4f). We found a peculiar structure which we assumed to be A $\beta$  aggregates by incubating in the presence of 10 or 50 mM of EPPS, respectively, for 1 day. These A $\beta$  aggregates seemed to be a coagulated form consisting of a lot of short fibrils. It was not observed before EPPS treatment or at a low concentration of EPPS. Interestingly, there were few fibrils in the surrounding areas of the large A $\beta$  aggregates. This looked like a surprisingly strong attraction force that is there to put short amyloid fibrils together in the same spot. Perhaps the strange attraction force could be enhanced as EPPS concentration increased, resulting in the reformation of larger A $\beta$  aggregates.

To scrutinize this phenomenon, we investigated the time-variant remodeling of the large A $\beta$  aggregates (Fig. 5). We imaged the A $\beta$  fibrils with EPPS with different incubation times such as 6, 12, and 24 h with 5 and 10 mM of EPPS (Fig. 5a-c, e-g). When treated with 5 mM of EPPS, the A $\beta$  fibrils were degraded for 12 h. Remarkably, the quantities of A $\beta$  fibrils were slightly increased for 24 h, albeit in the presence of EPPS. As the incubation time increased, the results of the surface roughness analysis also matched the AFM imaging results (Fig. 5d). More remarkably, the time for regeneration of A $\beta$  fibrils became 12 h earlier, and the reformation of the large A $\beta$  aggregates accelerated when 10 mM EPPS treated. Indeed, we once again observed large sized (4–6  $\mu$ m) of the large A $\beta$  aggregates that were similar to structures seen in Fig. 4c. As such, we verified our above-mentioned hypothesis, which meant that reformation of A $\beta$  aggregates was possible, despite the EPPS reaction. In addition, when the incubation time was 24 hours, the roughness of 10 mM EPPS treated sample increased 140 % than that of 5 mM EPPS treated sample (Fig. 5h). These results indicate that treatment of high concentrations of EPPS can lead to reform more densely aggregates than the original fibril or A $\beta$  aggregates.

To investigate how much the density of the large A $\beta$  aggregates depended on treated EPPS concentration, we analyzed the depths of height and amplitude error through AFM images for understanding the large A $\beta$  aggregates (Fig. 6). As shown the AFM images in Fig. 6a (10 mM of EPPS) and Fig. 6b

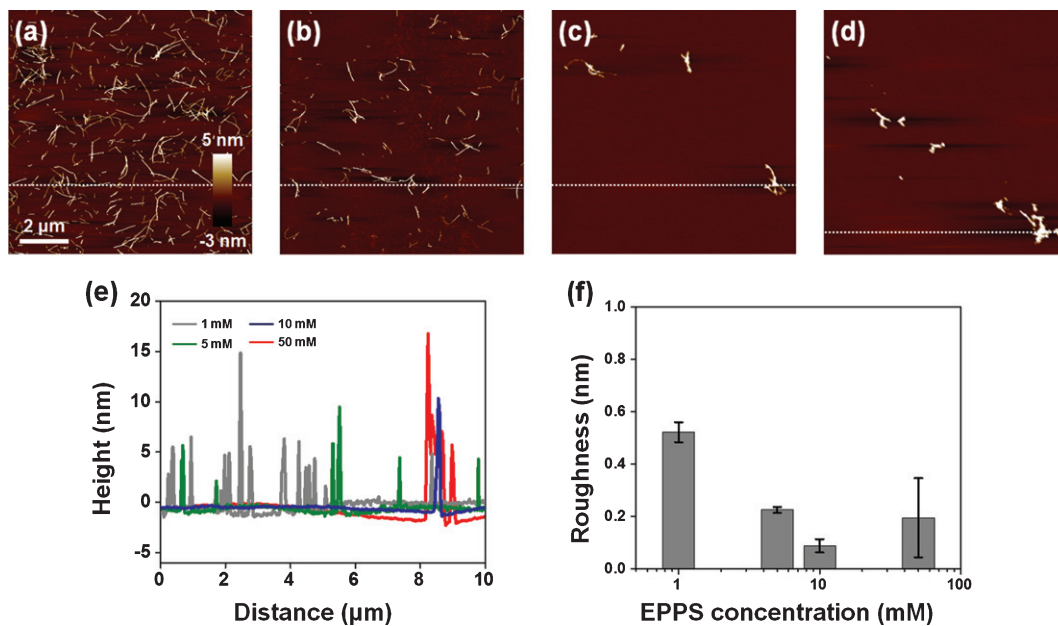


Fig. 2. AFM images of EPPS treated A $\beta$  fibrils (5  $\mu$ M) with different concentrations of EPPS (1–50 mM). (a) 1 mM of EPPS. (b) 5 mM of EPPS. (c) 10 mM of EPPS. (d) 50 mM of EPPS. Incubation time: 1 day. (e) Cross section profiles of A $\beta$  fibrils on images (a–d). We sectioned across the white dot line on images. (f) Differences of surface roughness by various EPPS treatment to A $\beta$  fibrils.

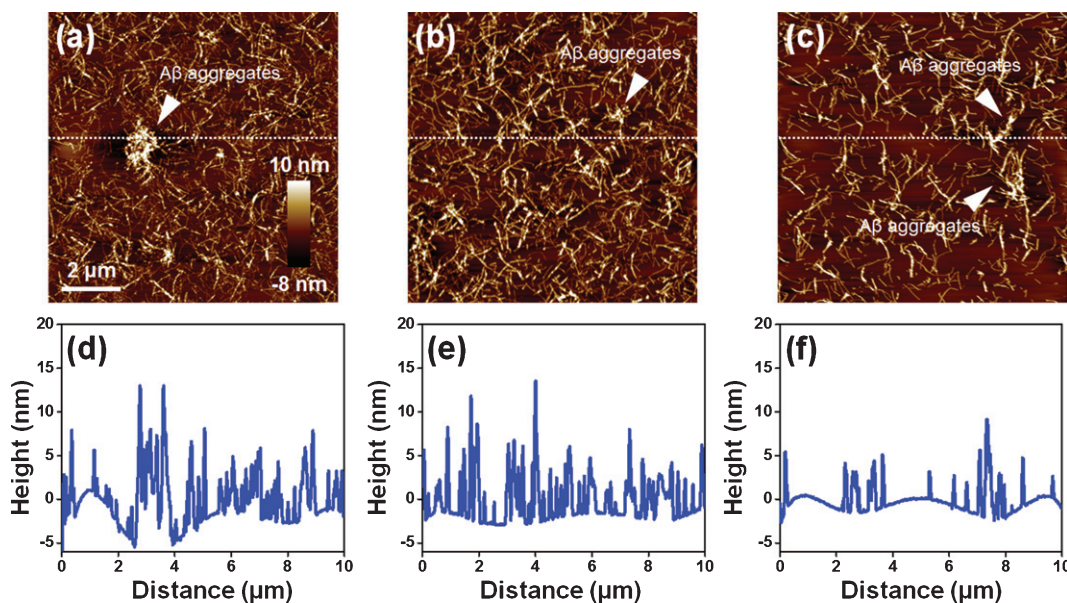


Fig. 3. AFM images of EPPS (1 mM) treated A $\beta$  fibrils (50  $\mu$ M) for different incubation times (1–3 days). (a) 1 day. (b) 2 days. (c) 3 days. White arrows indicate the A $\beta$  aggregates. (d–f) Cross section profiles of A $\beta$  fibrils on images (a–c). We sectioned across the white dot line on images.

(50 mM of EPPS), huge A $\beta$  aggregates can be formed at higher densities when a high concentration of EPPS is used to treat A $\beta$  fibrils. The depth of the height of the 50 mM-treated A $\beta$  aggregates was 2.3

times greater than that of the 10 mM-treated structure (Fig. 6c). In the same manner, amplitude error images (Fig. 6d, e) can give the best contrast between the large A $\beta$  aggregates and the substrate. The depth

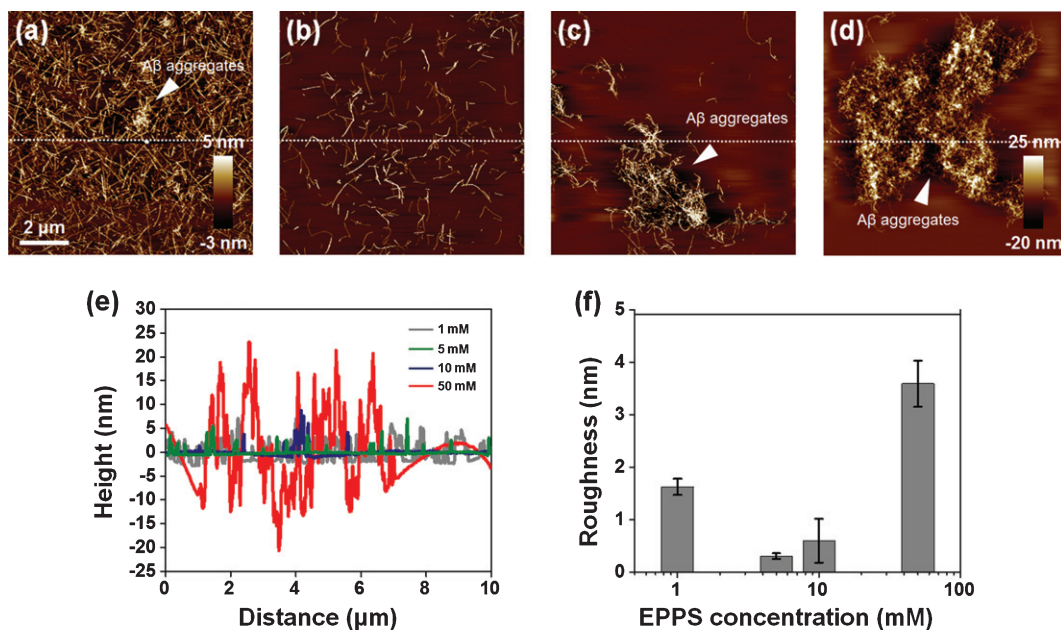


Fig. 4. AFM images of A $\beta$  fibrils (50  $\mu$ M) which are treated to different concentrations of EPPS (1–50 mM) for 1 day. (a) 1 mM of EPPS. (b) 5 mM of EPPS. (c) 10 mM of EPPS. (d) 50 mM of EPPS. White arrows indicate the A $\beta$  aggregates. We sectioned across the white dot line on images. (e) Cross section profiles of A $\beta$  aggregate on images (a–d). (f) Differences of surface roughness by various EPPS treatment to A $\beta$  fibrils.

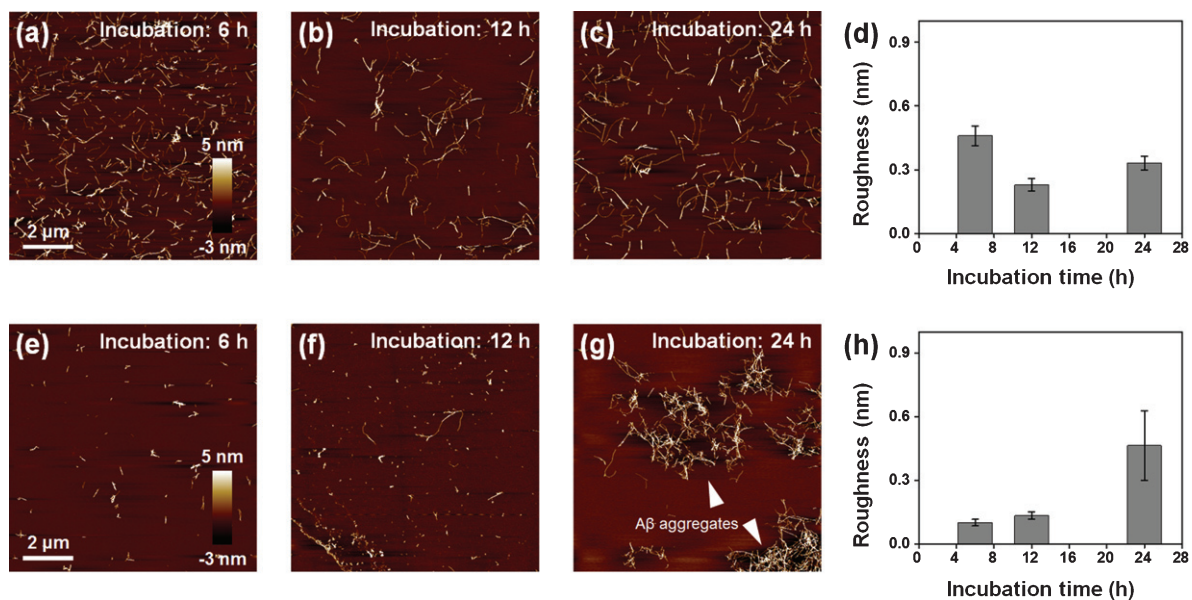


Fig. 5. AFM images of A $\beta$  fibrils (50  $\mu$ M) which are treated to EPPS for different incubation times (6–24 h) and concentrations of EPPS (5 and 10 mM). (a–c) 5 mM. (d) Differences of surface roughness by 5 mM EPPS treatment at different incubation time. (e–g) 10 mM. White arrow shows the A $\beta$  aggregates. (h) Differences of surface roughness by 10 mM EPPS treatment at different incubation time.

of the amplitude error of the 50 mM-treated A $\beta$  aggregates was 1.2 times greater than that of the 10 mM-treated structure (Fig. 6f). It was consistent with

the above-mentioned decomposition behavior of A $\beta$  fibrils and large A $\beta$  aggregates. Based on our data, we can propose a model describing the reformation

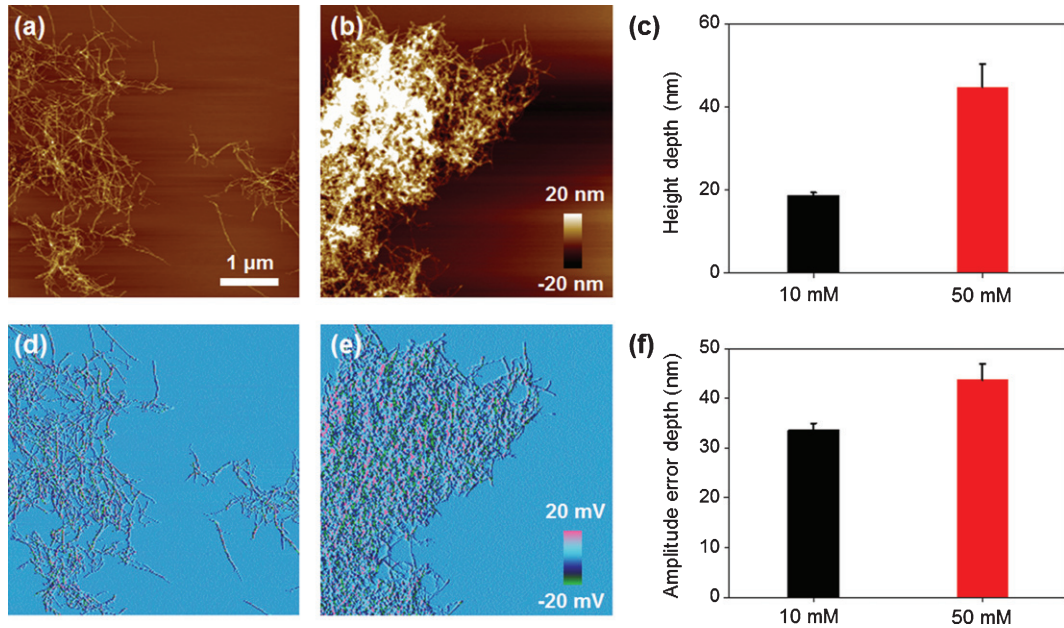


Fig. 6. Characterization of structural information of re-formed A $\beta$  aggregates depending on EPPS treatment by using AFM images. Topological images of A $\beta$  aggregates by (a) 10 and (b) 50 mM EPPS treatment for 1 day. (c) Average height depth of A $\beta$  aggregates. Amplitude error images of A $\beta$  aggregates by (d) 10 and (e) 50 mM EPPS treatment for 1 day. (f) Average amplitude error depth of A $\beta$  aggregates.

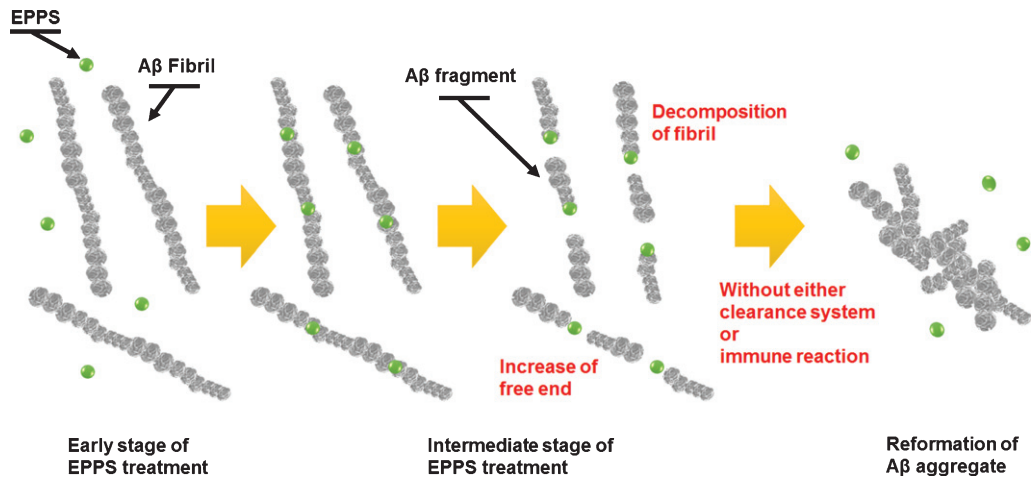


Fig. 7. Schematic diagram of our proposed model describing the mechanism of degradation and reformation of A $\beta$  aggregates.

mechanism of A $\beta$  aggregates in Fig. 7. At early stages of EPPS treatment, A $\beta$  fibrils degraded into shorter fibrils by direct binding of EPPS molecules to A $\beta$  fibrils. Because of no clearance event for the degraded A $\beta$  fragments, these fragments can coalesce through the free ends of broken fibrils. Concretely, as the number of free ends of degraded A $\beta$  fragment increases, it seems that each fibril fragment can be aggregated after further incubation.

Our results indicated that 1) EPPS was effective for degradation of A $\beta$  aggregates (consistent with prior studies), but the degradation was not perfect *in vitro* condition; 2) moreover, this imperfect degradation of A $\beta$  aggregates could cause the reformation of more A $\beta$  aggregates corresponding to larger sizes during the short incubation times; 3) therefore, EPPS treatment with the goal to cure AD should be done under well-controlled conditions. For example,

we hypothesize that AD patients who are dosed with EPPS should take a deep sleep, offering higher chances to activate the clearance system in the brain [23, 24]. We also anticipate an intermittent, but consecutive dosing EPPS to AD patients for long time (several years) potentially enabling complete degradation of all A $\beta$  aggregates degraded and excretion from the brain through a clearance system.

### Conclusions

In summary, we demonstrated AFM analysis of EPPS-driven degradation of A $\beta$  aggregates including fibrils and their aggregated form. We synthesized A $\beta$ <sub>1-42</sub> fibrils and treated to them with different concentrations of EPPS over various time periods. We found that EPPS worked very well in degrading preformed A $\beta$  aggregates, but the degradation did not mean perfect A $\beta$  elimination under the given conditions (e.g., *in vitro* system without clearance reactions). During the degradation process, tiny A $\beta$  aggregates were often found, which allowed for the reformation of A $\beta$  aggregates, regardless of the EPPS reactions. The problem was that the size of reformed A $\beta$  aggregates is much larger than their original forms. Moreover, the time for the reformation process was shortened, suggesting that the remained A $\beta$  fragments after EPPS treatment could act as seeds or nuclei for forthcoming A $\beta$  aggregation. Our findings will be useful for establishment of a proper EPPS prescription and for the discovery of more advanced, robust drugs for curing AD.

### ACKNOWLEDGMENTS

This work was supported by the National Research Foundation of Korea (NRF) grant funded by the Korean Government (MSIP) (No. NRF-2016R1A2B4010269). This research was also supported by Basic Science Research Program through the National Research Foundation of Korea (NRF) funded by the Ministry of Education (NRF-2017R1A6A3A11034311) and Korea University Grant.

### FINANCIAL DISCLOSURE

The authors have no conflict of interest to report.

### REFERENCES

- [1] Dobson CM (1999) Protein misfolding, evolution and disease. *Trends Biochem Sci* **24**, 329-332.
- [2] Merlini G, Bellotti V (2003) Molecular mechanisms of amyloidosis. *New Engl J Med* **349**, 583-596.
- [3] Blennow K, Hampel H, Weiner M, Zetterberg H (2010) Cerebrospinal fluid and plasma biomarkers in Alzheimer disease. *Nat Rev Neurol* **6**, 131-144.
- [4] Hardy J, Selkoe DJ (2002) The amyloid hypothesis of Alzheimer's disease: Progress and problems on the road to therapeutics. *Science* **297**, 353-356.
- [5] Bayliss D, Walsh JL, Shama G, Iza F, Kong MG (2009) Reduction and degradation of amyloid aggregates by a pulsed radio-frequency cold atmospheric plasma jet. *New J Phys* **11**, 115024.
- [6] Yagi H, Ozawa D, Sakurai K, Kawakami T, Kuyama H, Nishimura O, Shimanouchi T, Kuboi R, Naiki H, Goto Y (2010) Laser-induced propagation and destruction of amyloid  $\beta$  fibrils. *J Biol Chem* **285**, 19660-19667.
- [7] Lee W, Jung H, Son M, Lee H, Kwak TJ, Lee G, Kim CH, Lee SW, Yoon DS (2014) Characterization of the regrowth behavior of amyloid-like fragmented fibrils decomposed by ultrasonic treatment. *RSC Adv* **4**, 56561-56566.
- [8] Takeda T, Klimov DK (2008) Temperature-induced dissociation of A $\beta$  monomers from amyloid fibril. *Biophys J* **95**, 1758-1772.
- [9] Karran E, Mercken M, Strooper BD (2011) The amyloid cascade hypothesis for Alzheimer's disease: An appraisal for the development of therapeutics. *Nat Rev Drug Discov* **10**, 698-712.
- [10] Sacchettini JC, Kelly JW (2002) Therapeutic strategies for human amyloid diseases. *Nat Rev Drug Discov* **1**, 267-275.
- [11] Van Dam D, De Deyn PP (2006) Drug discovery in dementia: The role of rodent models. *Nat Rev Drug Discov* **5**, 956-970.
- [12] Wada M, Miyazawa Y, Miura Y (2011) A specific inhibitory effect of multivalent trehalose toward A $\beta$ (1-40) aggregation. *Polym Chem* **2**, 1822-1829.
- [13] Kim HY, Kim Y, Han G, Kim DJ (2010) Regulation of *in vitro* A $\beta$ 1-40 Aggregation mediated by small molecules. *J Alzheimers Dis* **22**, 73-85.
- [14] Kim HY, Kim HV, Jo S, Lee CJ, Choi SY, Kim DJ, Kim Y (2015) EPPS rescues hippocampus-dependent cognitive deficits in APP/PS1 mice by disaggregation of amyloid- $\beta$  oligomers and plaques. *Nat Commun* **6**, 8997.
- [15] Adamcik J, Jung J-M, Flakowski J, De Los Rios P, Dietler G, Mezzenga R (2010) Understanding amyloid aggregation by statistical analysis of atomic force microscopy images. *Nat Nanotech* **5**, 423-428.
- [16] Lee W, Lee H, Lee G, Yoon DS (2016) Advances in AFM imaging applications for characterizing the biophysical properties of amyloid fibrils. In *Exploring New Findings on Amyloidosis*, Fernandez-Escamilla A-M, ed. In Tech, Rijeka, p. Ch. 03.
- [17] Lee G, Lee W, Lee H, Lee CY, Eom K, Kwon T (2015) Self-assembled amyloid fibrils with controllable conformational heterogeneity. *Sci Rep* **5**, 16220.
- [18] Lee G, Lee W, Lee H, Lee SW, Yoon DS, Eom K, Kwon T (2012) Mapping the surface charge distribution of amyloid fibril. *Appl Phys Lett* **101**, 043703-043704.
- [19] Lee W, Kim I, Lee SW, Lee H, Lee G, Kim S, Lee SW, Yoon DS (2016) Quantifying L-ascorbic acid-driven inhibitory effect on amyloid fibrillation. *Macromol Res* **24**, 868-873.
- [20] Lee W, Lee H, Choi Y, Hwang KS, Lee SW, Lee G, Yoon DS (2017) Nanoelectrical characterization of amyloid- $\beta$  42 aggregates via Kelvin probe force microscopy. *Macromol Res* **25**, 1187-1191.

- [21] Smith JF, Knowles TPJ, Dobson CM, MacPhee CE, Welland ME (2006) Characterization of the nanoscale properties of individual amyloid fibrils. *Proc Natl Acad Sci U S A* **103**, 15806-15811.
- [22] Osorio RS, Pirraglia E, Agüera-Ortiz LF, During EH, Sacks H, Ayappa I, Walsleben J, Mooney A, Hussain A, Glodzik L, Frangione B, Martínez-Martín P, de Leon MJ (2011) Greater risk of Alzheimer's disease in older adults with insomnia. *J Am Geriatr Soc* **59**, 559-562.
- [23] Mawuenyega KG, Sigurdson W, Ovod V, Munsell L, Kasten T, Morris JC, Yarasheski KE, Bateman RJ (2010) Decreased clearance of CNS beta-amyloid in Alzheimer's disease. *Science* **330**, 1774.
- [24] Zuroff L, Daley D, Black KL, Koronyo-Hamaoui M (2017) Clearance of cerebral A $\beta$  in Alzheimer's disease: Reassessing the role of microglia and monocytes. *Cell Mol Life Sci* **74**, 2167-2201.